Nonlinear Modelling Approach for Linear Switched Reluctance Motor and its Validation by Two Dimensional FEA

I. Mahmoud, M. Fathallah, and H. Rehaoulia

Department of Electrical Engineering
National High School of Engineers of Tunis (ENSIT)
Tunisia University 5 av. Taha Hussein BP 56 – 1008 Tunis, Tunisia
Mahmoud.Imed@issatm.rnu.tn, Habib.Rahaoulia@esstt.rnu.tn

Abstract **─** This paper exposes two procedures in order to develop a refined analytical model which describes the behaviour of a linear switched reluctance motor. The first approach is based on the flux linkage and the second on the inductance, both versus position and current. Taking into account the non-linearity of the magnetic circuit, models are expressed by either Fourier series or polynomials where the only first three components are considered. Results of these analytical approaches are compared with those obtained using finite element methods (FEM) where a good agreement is observed.

Index Terms **─** Actuator, analytical model, computer simulation, electromagnetic force.

I. INTRODUCTION

Nowadays, linear switched reluctance machines are widely used. Unfortunately, in order to generate a high-propulsion force the LSRM must be operated in the saturation zone. In saturation conditions, main magnetic characteristics, such as flux linkage, inductance and propulsion force, are highly nonlinear. Consequently, the analytical methods based on some hypotheses are not very accurate to determine system performances and to elaborate control strategies. Regarding their modelling, there are many approaches such as lookup-table techniques, magnetic equivalent-circuit analysis, cubic-spline interpolations and finite-element methods (FEM), [3-4].

In a linear switched reluctance machine, the phase inductances and flux linkages vary with rotor position due to stator and rotor saliencies. The phase inductances and flux linkages at any rotor position also vary with the instantaneous phase currents because of magnetic saturation. However, these variations can be modelled analytically using the data obtained through FEM or through experiments. These analytical expressions are used to represent the linear switched reluctance machine dynamics and hence, the machine performance can be obtained, [1-2].

In order to determine a refined model which describes the behaviour of a saturated reluctant structure, there are basically two ways to represent the static LSRM characteristics. The first way is to plot the flux linkage versus rotor position and different phase currents. In this section, two approaches will be developed. The second way is to plot the phase inductance as function of rotor position and different phase currents, [5-8].

The paper is organized as follows. Taking apart the introduction and the conclusion, in Section 2, two approaches based on flux linkage model are developed. Section 3 gives the second method based on inductance model. Finally, Section 4 is reserved to determine the dynamic performances with and without saturation for the LSRM.

II. FLUX-LINKAGE-BASED MODEL OF LSRM

As previously stated, in a linear switched reluctance machine, the magnetic flux depends on both the relative stator and rotor position and winding current. Using Fourier series, the stator-phase flux linkage of the LSRM limited to the second harmonic order is:

$$\varphi(i,x) = \varphi_0 + \varphi_1 \cos\left(\frac{2\pi}{\lambda}x\right) + \varphi_2 \cos\left(\frac{4\pi}{\lambda}x\right). \quad (1)$$

For a given phase current, coefficients φ_0, φ_1 and φ_2 can be derived as functions of the aligned position flux linkage φ_c; the unaligned position flux linkage φ_{op} and the flux linkage at the midway φ_i, as follows, [9-10]:

$$\varphi_0 = \frac{1}{2}\left[\frac{1}{2}\left(\varphi_c + \varphi_{op}\right) + \varphi_i\right], \quad (2)$$

$$\varphi_1 = \frac{1}{2}\left(\varphi_c - \varphi_{op}\right), \quad (3)$$

$$\varphi_2 = \frac{1}{2}\left[\frac{1}{2}\left(\varphi_c + \varphi_{op}\right) - \varphi_i\right]. \quad (4)$$

Based on the above description, the proposed analytic modelling can be developed by using three curves: the aligned, the unaligned and the midway-position curves. The unaligned position curve, as shown in Fig. 1, is approximated by a straight line and can be described by:

$$\varphi_{op} = L_{op} i, \quad (5)$$

Submitted On: October 30, 2013
Accepted On: October 22, 2015

where L_{op} is a constant.

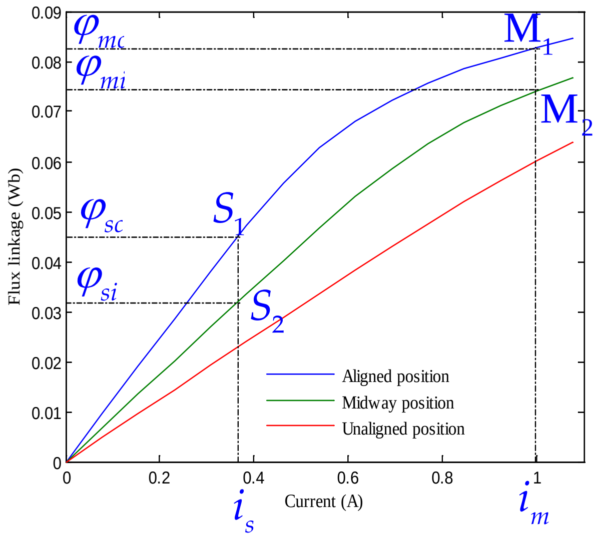

Fig. 1. Flux linkage against phase current for different mover positions.

To determine φ_c and φ_i and consequently the coefficients of the Fourier series φ_0, φ_1 and φ_2, two approaches have been developed.

A. First approach

Obviously, there is no linear relationship between the flux linkage and current in the saturated region for both aligned and midway positions, as shown in Fig. 1. At aligned and midway positions, the flux linkage may be approximated by an arctangent function:

$$\varphi_c = \frac{\arctan(a_1 i)}{a_2}, \tag{6}$$

$$\varphi_i = \frac{\arctan(m_1 i)}{m_2}, \tag{7}$$

where a_1, a_2, m_1 and m_2 are constants to be evaluated in the following sequence of steps.

- Step1: Choose two points φ_{mc} and φ_{sc} on the aligned position, Fig. 1. φ_{sc} is the flux linkage at the threshold saturated current i_s, and φ_{mc} is the flux linkage at the value of the triple to quadruple of i_m.
- Step 2: Constant a_1 is evaluated by using curve-fitting so that:

$$\frac{\varphi_{mc}}{\varphi_{sc}} = \frac{\arctan(a_1 i_m)}{\arctan(a_1 i_s)}. \tag{8}$$

- Step 3: Constant a_2 is calculated by:

$$a_2 = \frac{\varphi_{sc}}{\arctan(a_1 i_s)}. \tag{9}$$

- Step 4: Proceed the same way for m_1 and m_2.

Specifications of the designed prototype of the LSRM are shown in Fig. 2 and Table 1.

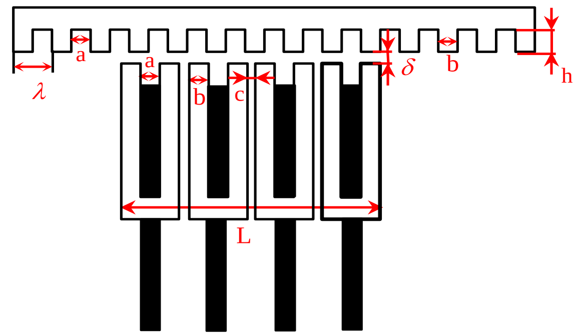

Fig. 2. Main dimensions of the conceived actuator.

Table 1: Motor mechanical and electrical parameters

Number of modules	4
Tooth width (b)	3 mm
Slot width (a)	3 mm
Tooth pitch (λ)	6 mm
Phase separation (c)	1.5 mm
Mover length	135 mm
Stator length (L)	40.5 mm
Air gap width (δ)	0.1 mm
Step size	1.5 mm
Number of turns per phase	520
Height of the mover teeth (h)	4 mm

Figure 3 shows the comparison of flux linkage versus phase current for different positions. We notice that the flux linkage versus current with different positions characteristics obtained by the proposed model closely match those obtained by FEM in the saturated region. However, the deviation in the linear region, as shown in Fig. 4, is obvious. Consequently, it is necessary to develop a new method to solve this problem.

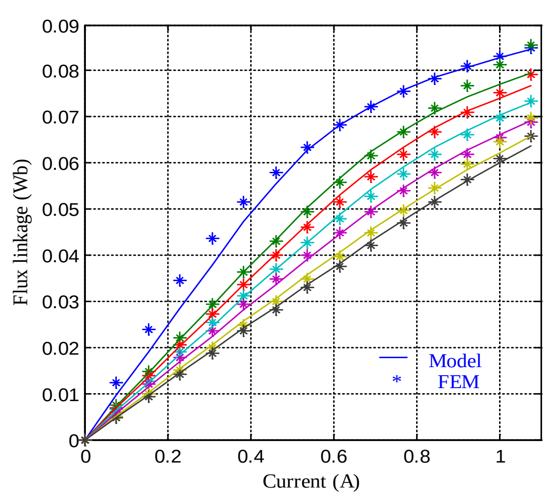

Fig. 3. Extreme left phase: comparison of flux linkage versus current with different positions (-Model, *FEM).

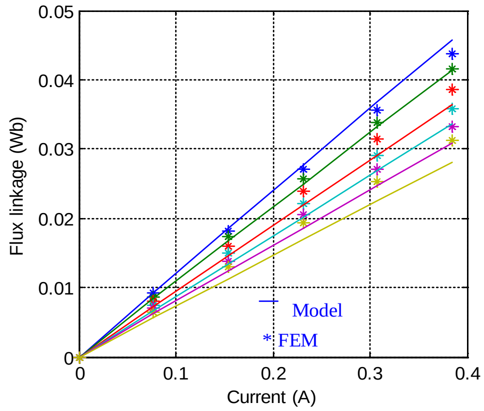

Fig. 4. Extreme left phase: comparison of flux linkage versus current with different positions in the linear region (-Model, *FEM).

B. Second approach

The flux linkage of the aligned position, shown in Fig. 1, can be expressed as, [11-17]:

$$\varphi_c = \begin{cases} L_c\, i & i \prec i_s \\ a_1 - \dfrac{a_2}{i} & i \geq i_s \end{cases}, \tag{10}$$

with

$$L_c\, i_s = a_1 - \frac{a_2}{i_s}. \tag{11}$$

In a similar way, we get for the midway position:

$$\varphi_i = \begin{cases} L_i\, i & i \prec i_s \\ m_1 - \dfrac{m_2}{i} & i \geq i_s \end{cases}, \tag{12}$$

with

$$L_i\, i_s = m_1 - \frac{m_2}{i_s}, \tag{13}$$

where L_c and L_i are also constants.

Constants a_1, a_2, m_1 and m_2 are evaluated by using respectively points M_1, S_1 and M_2, S_2 in Fig. 1.

Figure 5 gives the comparison of flux linkage produced by the left extreme phase versus current for different positions. It can be observed that results obtained by the proposed analytical model closely match those obtained by finite element methods.

The force produced by an LSRM is proportional to the rate of change of co-energy as the rotor moves from one position to another, as follows:

$$F(i,x) = \frac{\partial W_c(i,x)}{\partial x}, \tag{14}$$

$$W_c(i,x) = \int_0^i \varphi(i,x)\,di, \tag{15}$$

Using (14) and (15), we get:

$$F(i,x) = \int_0^i \frac{\partial \varphi(i,x)}{\partial x}\,di. \tag{16}$$

As shown previously, the electromagnetic force of the conceived motor is formulated by Equation (16). Now, the flux linkage is limited to the second order Fourier model as indicated by (1) and its related relations (2), (3) and (4). After necessary mathematical manipulations, it is not difficult to get, [18-19]:

$$F = -\frac{1}{2}\left[\frac{2\pi}{\lambda}\sin\left(\frac{2\pi}{\lambda}x\right)\right]\left[\int_0^i \varphi_c\,di - \int_0^i \varphi_{op}\,di\right] - \left[\frac{2\pi}{\lambda}\sin\left(\frac{4\pi}{\lambda}x\right)\right]\left[\frac{1}{2}\int_0^i \varphi_c\,di + \frac{1}{2}\int_0^i \varphi_{op}\,di - \int_0^i \varphi_i\,di\right]. \tag{17}$$

Electromagnetic force Equation (17) is a highly nonlinear function with respect to the mover position and current. Figure 6 represents the comparison of the thrust force produced by the left extreme phase as function of mover position. Characteristics are calculated via the proposed model and respectively by FEM. Evidently, the main difference comes from the choice of the mathematical model, specifically the linkage flux model, Equation (1). We expect that the accuracy may be improved by introducing higher order harmonics in Equation (1) and eventually by correctly choosing the number of Fourier terms.

Figure 6 shows a reasonable coincidence between the proposed analytical model with those obtained by the finite element method (FEM) which attests to the truth of the approach. Therefore, the second order of Fourier series is sufficient to achieve the desired results.

The flux linkage based model has larger error, but basically the results cover satisfactory in the second order of Fourier series. In order to improve these results, it was essential to develop a more realistic approach, [20-21].

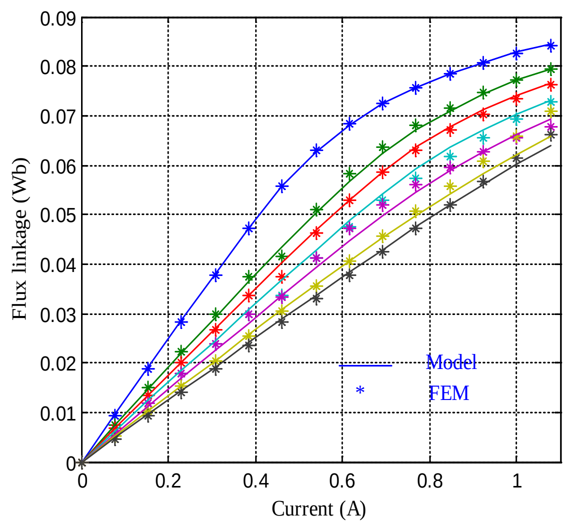

Fig. 5. Extreme left phase: comparison of flux linkage versus current with different positions (-Model, *FEM).

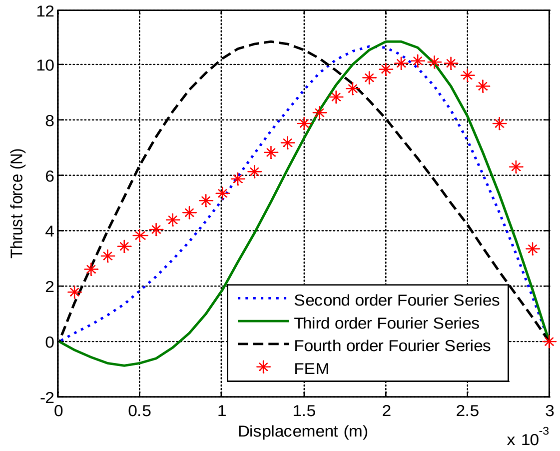

Fig. 6. Extreme left phase: comparison of the thrust force as function of mover position for different order of Fourier series (-Model, *FEM).

III. INDUCTANCE-BASED MODEL OF LSRM

In LSRM, the reluctance of the magnetic path in a given phase changes with rotor movement. The reluctance is maximum in unaligned position and minimum in the aligned position. As a consequence, phase inductance changes periodically as function of the rotor position. At any given rotor position, the phase inductance also varies with the instantaneous phase current. Therefore, the phase inductance versus mover position will be represented by Fourier series (18) and the nonlinear variation of its coefficients with current will be expressed by polynomial functions (20, 21), [22-23]:

$$L(x,i)=\sum_{k=0}^{m} L_k(i)\cos kN_r x \, , \tag{18}$$

where i, x and m are respectively the phase current, the position of the mover and the number of terms in the Fourier series.

The accuracy and stability of numerical simulations are the main challenges which should be met. To simplify expression (18), only the first three terms of the Fourier series are considered. The inductance expression is given by Equation (19), [24-25]:

$$\begin{aligned} L(x,i_j) &= L_0(i_j)+L_1(i_j)\cos(N_r(x-(j-1)\frac{2\pi}{NN_r})) \\ &+ L_2(i_j)\cos(2N_r(x-(j-1)\frac{2\pi}{NN_r})) \end{aligned} \, , \tag{19}$$

with $L(x, i_j)$ and N are respectively the inductance associate to the phase j in the position x of the mover for the current i_j and the number of phase.

To determine the three coefficients L_0, L_1 and L_2, we use the inductance at three positions: aligned position L_c (i_j), unaligned position L_{op} (i_j) and midway position between the above two positions L_i (i_j). Note that, L_{op} (i_j) can be treated as a constant but, L_c (i_j) and L_i (i_j) are functions of the phase current i_j and can be approximated by the polynomials, [25-26]:

$$L_c(i_j)=\sum_{n=0}^{p} a_n i^n{}_j \, , \tag{20}$$

$$L_i(i_j)=\sum_{n=0}^{p} b_n i^n{}_j \, , \tag{21}$$

where p is the order of the polynomials and a_n, b_n are the coefficients.

In our research, $p = 6$ is chosen after we compare the fitting results of different p values, (p = 3, p = 4, p = 5 and p = 6 have been tried and compared). As a result the inductance of the aligned position L_c (i_j) and midway position L_i (i_j) are approximated respectively by the Equations (22) and (23). Figure 7 shows the good agreement between the FEM and the proposed curve fitting methods. FEM results are obtained by Magnet 2D software. Analytical calculations were performed by means of curve-fitting matlab toolbox:

$$\begin{aligned} &L_c(i)=a_1 i^6+a_2 i^5+a_3 i^4+a_4 i^3+a_5 i^2+a_6 i+a_7 \\ &a_1=-0.4883 \quad a_2=1.356 \\ &a_3=-1.153 \quad a_4=0.1993 \\ &a_5=0.06603 \quad a_6=-0.02222 \\ &a_7=0.1253 \end{aligned} \, , \tag{22}$$

$$\begin{aligned} &L_i(i)=b_1 i^6+b_2 i^5+b_3 i^4+b_4 i^3+b_5 i^2+b_6 i+b_7 \\ &b_1=-0.3227 \quad b_2=1.186 \\ &b_3=-1.609 \quad b_4=0.9716 \\ &b_5=-0.2766 \quad b_6=0.03345 \\ &b_7=0.09355 \end{aligned} \, . \tag{23}$$

Consequently, the three coefficients for the Fourier series can be computed as, [27-29]:

$$L_0=\frac{1}{2}\left[\frac{1}{2}\left(L_c+L_{op}\right)+L_i\right], \tag{24}$$

$$L_1=\frac{1}{2}\left(L_c-L_{op}\right), \tag{25}$$

$$L_2=\frac{1}{2}\left[\frac{1}{2}\left(L_c+L_{op}\right)-L_i\right]. \tag{26}$$

The stator phase inductance at the aligned position is very affected by the stator phase current variations. On the contrary, the unaligned inductance is practically constant due to the large reluctance that characterizes this position.

It is worth mentioning that, found analytical model remains valid for any position x and any current i as illustrated by Figs. 8 and 9.

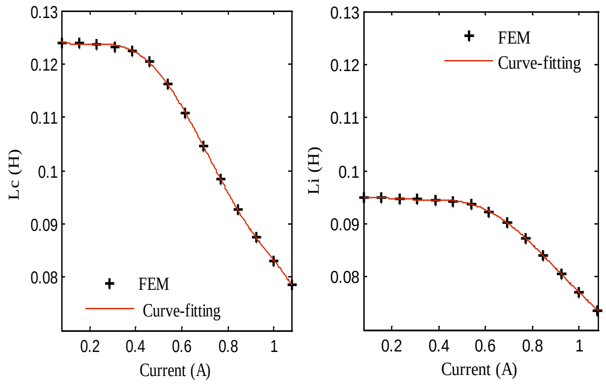

(a) (b)

Fig. 7. Evolution of the winding inductance versus current: (a) aligned position, and (b) midway position.

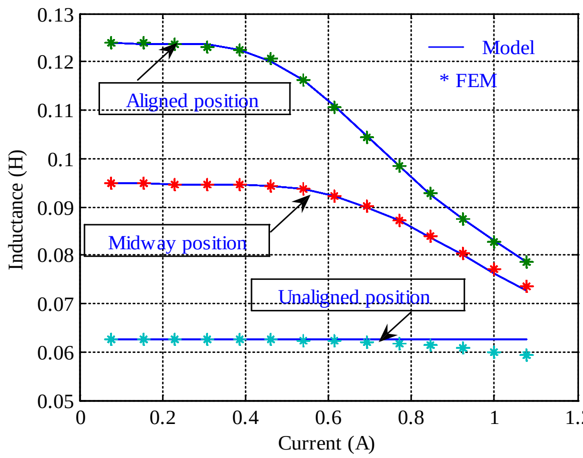

Fig. 8. Extreme left phase: comparison of inductance versus current with three positions (-Model, *FEM).

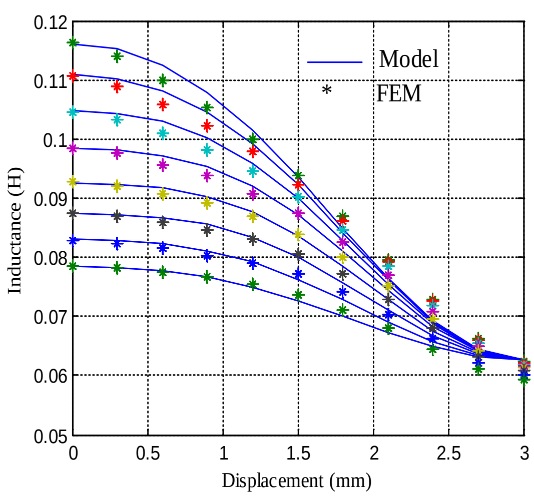

Fig. 9. Extreme left phase: comparison of inductance versus position with different currents (-Model, *FEM).

Multiplying the expression of inductance by the current (i), it gives the expression of linkage flux, [30-32]:

$$\varphi(i,x) = iL(i,x). \tag{27}$$

Figure 10 gives the comparison of linkage flux produced by the left extreme phase versus current for different positions. It can be observed that the linkage flux versus current for different position characteristics which are obtained by the proposed model closely match those obtained by finite element methods. These results prove the effectiveness of the proposed model.

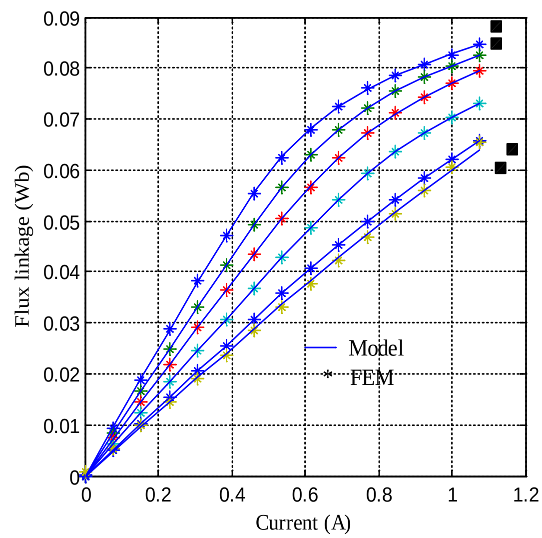

Fig. 10. Extreme left phase: comparison of linkage flux versus current with different positions (-Model, *FEM).

Furthermore, it is well known that the total electromagnetic force is given by the following expression:

$$F = \sum_{j=1}^{N} F_j(i,x), \tag{28}$$

where N is the number of phase, F_j the force of phase j and i_j the phase current. Consequently, the force F_j can be described by the following equation:

$$F_j(i,x) = \frac{\partial W_{c,j}}{\partial x} = \frac{\partial\left(\int_0^i L(x,i_j)\, i_j di_j\right)}{\partial x}, \tag{29}$$

L (x, i_j) is the inductance associate to the phase j in the position x of mover for the current i_j.

For a given current, Equation (29) becomes:

$$F_j(i,x) = \frac{1}{2}\frac{\partial L_j(x)}{\partial x} i_j^2 \Big|_{[i]=cte}. \tag{30}$$

Figure 11 shows also a reasonable coincidence between the curve obtained by the proposed model and that taken via the finite element method (FEM).

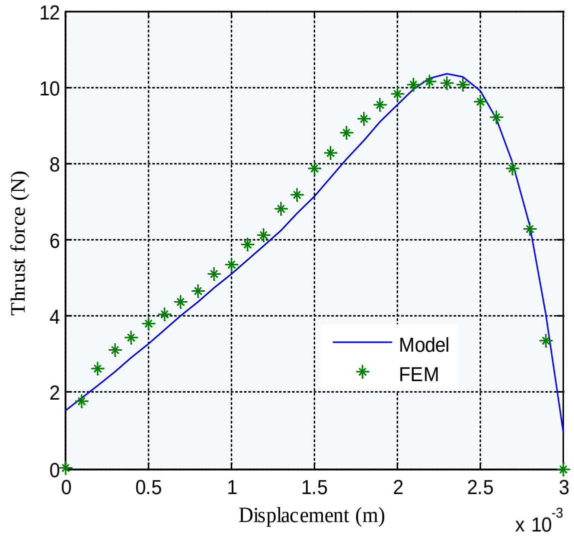

Fig. 11. Extreme left phase: comparison of the thrust force as function of mover position (-Model, *FEM).

IV. DYNAMIC PERFORMANCES OF LSRM

We plan to study the dynamic behavior of the all biomedical system. Dynamic electric equations of the four phases are:

$$U_A = Ri_A + \left(L(x,i_A) + \frac{\partial L(x,i_A)}{\partial i_A} i_A \right) \frac{d\,i_A}{dt} + \frac{\partial L(x,i_A)}{\partial x} i_A \frac{dx}{d\,t}, \quad (31)$$

$$U_B = Ri_B + \left(L(x,i_B) + \frac{\partial L(x,i_B)}{\partial i_B} i_B \right) \frac{d\,i_B}{dt} + \frac{\partial L(x,i_B)}{\partial x} i_B \frac{dx}{d\,t}, \quad (32)$$

$$U_C = Ri_C + \left(L(x,i_C) + \frac{\partial L(x,i_C)}{\partial i_C} i_C \right) \frac{d\,i_C}{dt} + \frac{\partial L(x,i_C)}{\partial x} i_C \frac{dx}{d\,t}, \quad (33)$$

$$U_D = Ri_D + \left(L(x,i_D) + \frac{\partial L(x,i_D)}{\partial i_D} i_D \right) \frac{d\,i_D}{dt} + \frac{\partial L(x,i_D)}{\partial x} i_D \frac{dx}{d\,t}. \quad (34)$$

The mechanical equation relating the rotor acceleration, speed, position and load force is:

$$m_c \frac{dx^2}{dt^2} = F\left(x\right) - \xi \frac{dx}{dt} - F_0 signe\left(\frac{dx}{dt}\right) - F_r, \quad (35)$$

parameters m_c, ξ, F_0 and F_r designate the actuator mass, the viscous friction force, the dry friction force and the load force.

In order to validate the accuracy of the proposed model, Matlab/Simulink was used to perform the simulation with this model. This last, has been tested and compared by the linear model to predict the dynamic performance of the LSRM. Dynamic behaviour of position, thrust force and speed are resumed in Fig. 12. Note that, the excitation of phase A allows positioning the translator on the first step corresponding to 1.5 mm. Successive excitation of other phases are needed for next steps.

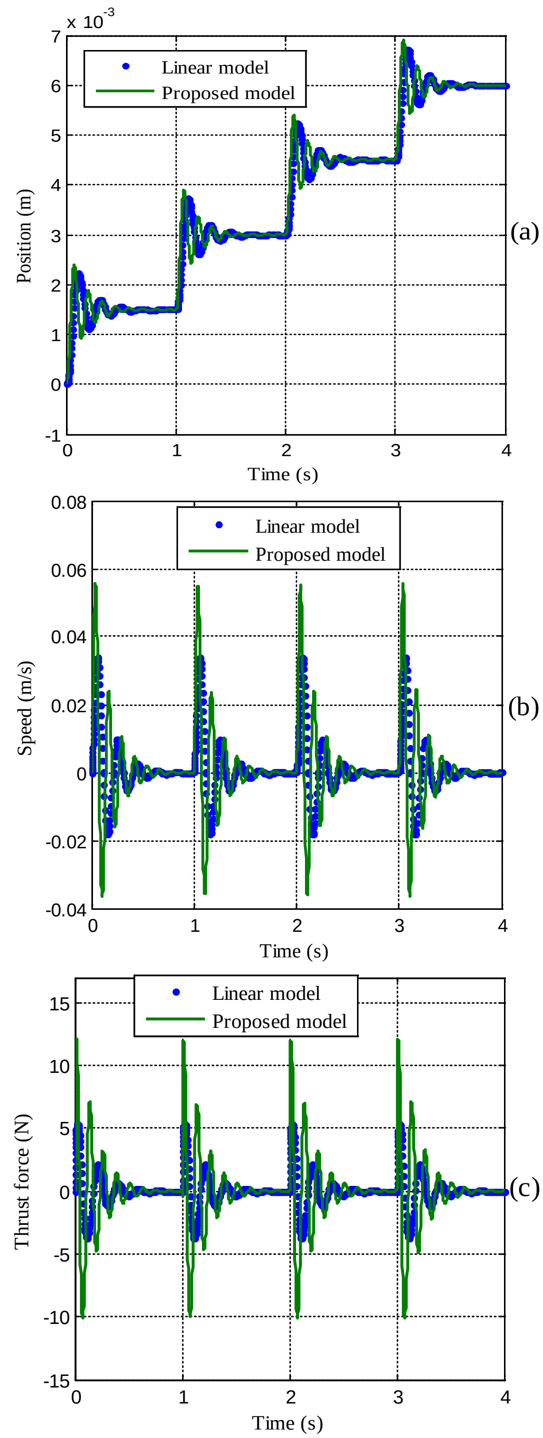

Fig. 12. (a) Position, (b) speed, and (c) thrust force evolution during four steps (*****linear model, **-**proposed model).

The proposed model of the LSRM is characterized by a strongly oscillatory translation compared to the linear model. These oscillations are expected to disturb the accuracy of the position and the constancy speed often required by many industrial applications and especially in the medical fields. This problem often leads to losses of synchronism, [33-36].

V. CONCLUSION

It is essential to have an accurate model of a linear switched reluctance motor that describes its static characteristics. It has been shown in this paper that there are different ways of modelling static characteristics of an LSRM. The developed analytical models consider the variation of either the phase flux linkage or the phase inductance with rotor position accounting for magnetic saturation. Results are compared to those obtained via the 2D-FEM. The comparison shows a reasonable agreement, proving the validity of the proposed approaches.

REFERENCES

[1] G. Singh, "Modelling and dynamic simulation of multiple-stack variable-reluctance step motors," *Comput. and Elect. Engng*., vol. 1, pp. 481-500, 1974.

[2] M. Feyrouz, "Contribution à l'Etude d'une Génératrice à Réluctance Variable," *Magistère en Electrotechnique*, Université Mentouri de Constantine, 2009.

[3] F. R. Salmasi, "Virtual auto-tuning position and torque sensors for switched reluctance motor drives," *IEEE Transactions on Industry Applications*, pp. 1355-1361, 2004.

[4] H. P. Chi, "Simplified flux-linkage model for switched-reluctance motors," *IEE Proc. - Electr. Power Appl.*, vol. 152, no. 3, pp. 577-583, May 2005.

[5] S. W. Zhao, "A self-tuning regulator for high-precision position control of linear switched reluctance motor," *IEEE Transactions on Industrial Electronics*, vol. 54, no. 5, Oct. 2007.

[6] J. Nicholas, "Modeling of a saturated switched reluctance motor using an operating point analysis and the unsaturated torque equation," *IEEE Transactions on Industry Applications*, vol. 36, no. 3, May/June 2000.

[7] M. Imed and R. Habib, "Development of analytical approach for linear switched reluctance motor and its validation by two dimensional FEA," *International Conference on Control, Engineering & Information Technology (CEIT'14)*, Monastir – Tunisia, Mar. 22-25, 2014.

[8] J. Hur, "Modeling of switched reluctance motor using Fourier series for performance analysis," *Journal of Applied Physics*, 2003.

[9] V. Ioan-Adrian, "Analytical flux linkage model of switched reluctance motor," *Rev. Roum. Sci. Techn. – Électrotechn. et Énerg*., vol. 54, no. 2, pp. 139-146, Bucarest, 2009.

[10] I. A. Viorel, "Speed-thrust control of a double sided linear switched reluctance motor (DSL-SRM)," *Proceedings of the 2008 International Conference on Electrical Machines*, Paper ID 879, 978-1-4244-1736-0/08 ©2008 IEEE, 2008.

[11] L. Lawler, "A simulation model for the four phase switched-reluctance motor," *Thesis, The University of Tennessee*, Knoxville, May 2003.

[12] Z. Haijuin, "Static characteristic and vibration dynamic response analysis of switched reluctance motor system," *International Conference on Mechatronics and Automation, Proceeding of IEEE*, Aug. 2009.

[13] H. Jin, "Modelling of switched reluctance motor using Fourier series for performance analysis," *Journal of Applied Physics*, vol. 93, no. 10, 15, May 2003.

[14] H. P. Chi, "Flux-linkage based models for switched-reluctance motors," *Ph.D. Philosophy, National Cheng Kung University*, Dec. 2005.

[15] A. O. Khalil, "Modeling and analysis of four quadrant sensorless control of a switched reluctance machine over the entire speed range," *The Graduate Faculty of the University of Akron, Ph.D. Thesis*, Aug. 2005.

[16] J. Lee, "Structural design optimization of electrical motors to improve torque performance," *Ph.D. Thesis, University of Michigan*, 2010.

[17] I. G. Sirbu, "Novel approach for electromagnetic actuators analysis in transient behaviour," *Advances in Electrical and Computer Engineering*, vol. 12, no. 1, 2012.

[18] E. Pădurariu, "Switched reluctance motor analytical models, comparative analysis," *The International Conference on Optimization of Electrical and Electronic Equipment, OPTIM 2010*, IEEE, 2010.

[19] R. M. Schupbach, "Modeling switched reluctance motors under multi-phase excitation," *University of Arkansas*, Department of Electrical Engineering 3217 Bell Engineering Center Fayetteville, AR 72701 – 1201 (501) 575-3005, Second Annual Report - Part 1 (AR2.1).

[20] A. Espírito Santo, "Static simulation of a linear switched reluctance actuator with the flux tube method," *Advances in Electrical and Computer Engineering*, vol. 10, no. 2, 2010.

[21] N. C. Lenin, "Force profiles of a linear switched reluctance motor having special pole face shapes," *Advances in Electrical and Computer Engineering*, vol. 10, no. 4, 2010.

[22] S. Song, "A comparative study on modeling methods for switched reluctance machines," *Computer and Information Science*, vol. 3, no. 2, May 2010.

[23] K. Ha, "Position estimation in switched reluctance

motor drives using the first switching harmonics of phase voltage and current," *Ph.D. Thesis, Virginia Polytechnic Institute and State University*, 2008.

[24] B. Fahimi, "A new approach to model switched reluctance motor drive application to dynamic performance prediction, control and design," C*onference IEEE 1998*, 0-7803-4489-8/98, 1998.

[25] W. Lu, "Modelling and control of a switched reluctance machine for electro-mechanical brake systems," *Ph.D. Thesis, Ohio State University*, 2005.

[26] J. Maridor, "Design, optimization, and sensorless control of a linear actuator," *Ph.D. Thesis, école Polytechnique Fédérale de Lausanne*, 2011.

[27] H. Gao, "Inductance model-based sensorless control of the switched reluctance motor drive at low speed," *IEEE Transactions on Power Electronics*, vol. 19, no. 6, Nov. 2004.

[28] K. I. Hwu, "Applying Powersys and Simulink to modeling switched reluctance motor," *Tamkang Journal of Science and Engineering*, vol. 12, no. 4, pp. 429-438, 2009.

[29] H. Torkaman, "Comprehensive detection of eccentricity fault in switched reluctance machines using high frequency pulse injection," *IEEE Transactions on Power Electronics*, vol. 28, no. 3, 1382{1390, 2013.

[30] E. K. Beser, "Design and analysis of an axially laminated reluctance motor for variable-speed applications," *Advances in Electrical and Computer Engineering*, vol. 13, no. 1, 2013.

[31] H. Torkaman, "Comprehensive detection of eccentricity fault in switched reluctance machines using high frequency pulse injection," *IEEE Transactions on Power Electronics*, vol. 28, no. 3, 1382{1390, 2013.

[32] I. G. Sirbu, "Novel approach for electromagnetic actuators analysis in transient behavior," *Advances in Electrical and Computer Engineering*, vol. 12, no. 1, 2012.

[33] A. Mosallanejad and A. Shoulaie, "Inductance profile calculation of step winding structure in tubular linear reluctance motor using three dimensional finite element method," *Euro. Trans. Electr. Power*, vol. 22, pp. 721-732, 2012.

[34] S. Méndez, "Design, characterization, and validation of a 1-kW AC self-excited switched reluctance generator," *IEEE Transactions on Industrial Electronics*, vol. 61, no. 2, Feb. 2014.

[35] J. F. Pan, Y. Zou, and G. Cao, "Adaptive controller for the double-sided linear switched reluctance motor based on the nonlinear inductance modelling," *IET Electr. Power Appl.*, vol. 7, iss. 1, pp. 1-15, 2013.

[36] S. Song, "Accurate measurement and detailed evaluation of static electromagnetic characteristics of switched reluctance machines," *IEEE Transactions on Instrumentation and Measurement*, vol. 64, no. 3, Mar. 2015.

Imed Mahmoud was born in Mahdia, Tunisia, on March 4, 1982. He received the Diploma of Baccalaureate in Applied Science degree in 2002 at Secondary School Souassi Mahdia, the M.Sc. degree in 2006, in Electrical Engineering option Electrical Engineering and Power Electronics and Master degree in Electrical Engineering and Systems Industrial 2008 all from the ESSTT (High School of Sciences and Technology of Tunis), University of Tunis, Tunisia. He joined the teaching staff of the ESSTT in 2008. His main research interests are study, design, modelling and control of linear actuators.

Mourad Fathallah Assistant Professor in Electrical Engineering at the ENISO. He is a doctor in Electrical Engineering INSA Lyon. He has five years experience in Consulting in Parisian society (Speech at multiple clients: VALEO, Barco, Philips etc.). Projects in Electronics (databases, design of control modules fluorescent lamps (subject to patent), size of losses in power lamps.

Habib Rehaoulia received the B.S. degree in 1978, the M.S. degree in 1980 and the Doctoral degree in 1983, all from the ENSET (Institute of Technical Sciences), University of Tunis, Tunisia. He joined the teaching staff of the ENSET in 1978. Since 1995, he is with the ESSTT (Institute of Sciences and Technology of Tunis), where he obtained the Habilitation degree in 2007.

During his career, he was on leave for several months at WEMPEC (University of Madison Wisconsin USA), ENSIEG (University of Grenoble France), "Lab. d'électrotechnique" (University of Paris VI France), and the CREA (University of Picardie France). His main research interests are analysis, modeling and simulation of electrical machines.

Rehaoulia is a Member of SIME (Signal, Image and Energy Management), ASET (Association for Tunisian Electrical Specialists), ATTNA (Tunisian Association for Numerical Techniques and Automatics) and IEEE (region 8, France section).